EBioMedicine 5 (2016) 59–67

Contents lists available at ScienceDirect

EBioMedicine

journal homepage: www.ebiomedicine.com

Research Paper

CD8$^+$ T-cell Immune Evasion Enables Oncolytic Virus Immunotherapy

Aldo Pourchet [a], Steven R. Fuhrmann [e], Karsten A. Pilones [b,1], Sandra Demaria [b,d,1], Alan B. Frey [c,d], Matthew Mulvey [e,*], Ian Mohr [a,d,*]

[a] Department of Microbiology, New York University School of Medicine, New York, NY, USA
[b] Department of Pathology, New York University School of Medicine, New York, NY, USA
[c] Department of Cell Biology, New York University School of Medicine, New York, NY, USA
[d] NYU Cancer Institute, New York University School of Medicine, New York, NY, USA
[e] Benevir Biopharm, Gaithersburg, MD, USA

ARTICLE INFO

Article history:
Received 28 September 2015
Received in revised form 8 January 2016
Accepted 15 January 2016
Available online 19 January 2016

Keywords:
Oncolytic virus
Immunotherapy
TAP inhibitor
CD8$^+$ T-cell immune evasion

ABSTRACT

Although counteracting innate defenses allows oncolytic viruses (OVs) to better replicate and spread within tumors, CD8$^+$ T-cells restrict their capacity to trigger systemic anti-tumor immune responses. Herpes simplex virus-1 (HSV-1) evades CD8$^+$ T-cells by producing ICP47, which limits immune recognition of infected cells by inhibiting the transporter associated with antigen processing (TAP). Surprisingly, removing ICP47 was assumed to benefit OV immuno-therapy, but the impact of inhibiting TAP remains unknown because human HSV-1 ICP47 is not effective in rodents. Here, we engineer an HSV-1 OV to produce bovine herpesvirus UL49.5, which unlike ICP47, antagonizes rodent and human TAP. Significantly, UL49.5-expressing OVs showed superior efficacy treating bladder and breast cancer in murine models that was dependent upon CD8$^+$ T-cells. Besides injected subcutaneous tumors, UL49.5-OV reduced untreated, contralateral tumor size and metastases. These findings establish TAP inhibitor-armed OVs that evade CD8$^+$ T-cells as an immunotherapy strategy to elicit potent local and systemic anti-tumor responses.

1. Introduction

Emergent biological therapies may command tremendous advantages over traditional cancer chemotherapy and radiation, whose efficacies are restricted by toxicity and resistance. Besides reduced toxicity and greater selectivity for tumor cells, new therapies reliant on multiple methods of cell killing distinct from conventional antineoplastic agents and capable of eliciting systemic anti-tumor immune responses promise durable cures and overall survival benefits (Liu et al., 2007). Capitalizing on their inherent ability to invade cells, reprogram them to produce infectious progeny, and spread, viruses can be tailored to selectively destroy tumor cells by modifying their genomes (Bell and McFadden, 2014; Lichty et al., 2014; Chiocca and Rabkin, 2014; Brown et al., 2014). The resulting engineered viruses are attenuated due to deletion of key virulence genes, yet retain the ability to replicate productively in and destroy cancer cells. Such variants, which do not cause disease but are selectively virulent in tumors are termed *oncolytic viruses* (*OVs*). Tumor destruction driven, in part, by active viral replication within cancer cells is referred to as viral oncolysis (Bell and McFadden, 2014; Lichty et al., 2014; Chiocca and Rabkin, 2014; Brown et al., 2014). In addition to direct oncolytic action, OVs stimulate systemic, anti-tumor immune responses and are likewise potent immunotherapeutic agents (Lichty et al., 2014; Chiocca and Rabkin, 2014; Brown et al., 2014; Dharmadhikari et al., 2015; Kaufman et al., 2015).

OV platforms using herpes simplex virus-1 (HSV-1) are particularly encour-aging in part because the virus replicates in a range of tumors and is effectively attenuated by deleting the $\gamma_1$34.5 neuropathogenesis genes (Chou et al., 1990). Furthermore, independent $\gamma_1$34.5-deficient (Δ34.5) HSV-1 strains have proven safe in human clinical trials (Rampling et al., 2000; Markert et al., 2000; Hu et al., 2006; Senzer et al., 2009; Harrington et al., 2010; Andtbacka et al., 2015). Along with viral oncolysis, HSV-1 OVs generate systemic anti-tumor immune responses upon local administration (Toda et al., 1999; Liu et al., 2003). Nevertheless, serious deficiencies in the design of present generation OVs remain, many of which lack functions to evade host innate or acquired immune defenses (Ikeda et al., 1999; Wang et al., 2003; Fulci et al., 2006; Haralambieva et al., 2007; Nguyên et al., 2008; Zamarin et al., 2009; Altomonte et al., 2009; Le Bœuf et al., 2013). Notably, although wild-type HSV-1 replicates in hosts and naturally evades pre-existing innate and acquired immune responses (Posvad and Rosenthal, 1992; Koelle et al., 1993; York et al., 1994), a key immune evasion gene was deleted in some modified Δ34.5 OVs (Taneja et al., 2001; Todo et al., 2001; Liu et al., 2003) and deleting $\gamma_1$34.5 genes

* Corresponding authors.
E-mail addresses: Matt@benevir.com (M. Mulvey), ian.mohr@med.nyu.edu (I. Mohr).
[1] Present address: Dept of Radiation Oncology, Weill Cornell Medical College, New York, NY, United States.

http://dx.doi.org/10.1016/j.ebiom.2016.01.022

results in OVs unable to counteract innate defenses (Mohr and Gluzman, 1996; Mulvey et al., 1999, 2004), severely restricting direct OV cell-killing (Taneja et al., 2001; Todo et al., 2001; Liu et al., 2003) and potentially impairing indirect induction of systemic antitumor immune responses.

To counteract innate, cell intrinsic host defenses that limit Δ34.5 OV replication within tumors, variants were isolated that expressed the HSV-1 Us11 protein, normally produced late in the lifecycle, at immediate-early (IE) times (Mohr and Gluzman, 1996; Mulvey et al., 1999). Remarkably, Δ34.5 OVs expressing IE Us11 remained neuroattenuated (Mohr et al., 2001), but effectively countered interferon-induced, cell-intrinsic anti-viral responses (Mulvey et al., 1999, 2004), replicated substantially better within tumors, and were more effective anti-tumor agents in pre-clinical studies (Taneja et al., 2001; Todo et al., 2001; Liu et al., 2003). Indeed, a related Δ34.5, IE Us11-expressing HSV-1 has completed US phase III trials (Andtbacka et al., 2015; Dolgin, 2015) and a biologics license application recently approved by the FDA (http://www.fda.gov./BiologicsBloodVaccines/CellularGeneTherapyProducts/ApprovedProducts/ucm469411.htm). However, the genetic alteration enabling IE-Us11 expression also deleted the neighboring HSV1 gene encoding the ICP47 immunomodulator (Mohr and Gluzman, 1996; He et al., 1997; Mulvey et al., 1999; Taneja et al., 2001; Todo et al., 2001; Liu et al., 2003). By inhibiting TAP, ICP47 down-regulates cell surface MHC class I expression and allows HSV-1 to complete its productive growth program despite the presence of host anti-HSV-1 $CD8^+$ T-cells (Früh et al., 1995; Hill et al., 1995). Without ICP47, increased clearance of infected cells by $CD8^+$ T-cells could severely restrict OV spread through the tumor impacting both direct oncolysis and anti-tumor immune response development. This limitation is likely critical given the prevalence of HSV-1 seropositive individuals, the rapid seroconversion of sero-negative patients after HSV-1 OV exposure (Hu et al., 2006), and the finding that evading $CD8^+$ T-cells facilitates herpesvirus super-infection of seropositive hosts (Hansen et al., 2010). Surprisingly, both the role of $CD8^+$ T-cell evasion and how viral immuno-modulators impact OV therapy remain unknown in part because human HSV-1 ICP47 has a low affinity for rodent TAP, impairing proper assessment of its biological function in rodent models (Ahn et al., 1996; Tomazin et al., 1996). Moreover, while removing the viral TAP inhibitor was proposed to benefit OV therapy by improving its immune stimulating properties, a direct comparison of how TAP inhibition impacts OV efficacy was never performed (Liu et al., 2003; Dolgin, 2015). Here, we address this problem by isolating an HSV-1 OV armed with the bovine herpesvirus 1 (BHV-1) TAP-inhibitor (UL49.5), which unlike its HSV-1 analog, antagonizes rodent and human TAP (Koppers-Lalic et al., 2005; Verweij et al., 2011a). Significantly, UL49.5-expressing OVs showed superior efficacy treating bladder and breast cancer in murine pre-clinical models that was dependent upon a $CD8^+$ T-cell response. In addition to treating directly injected, subcutaneous (*sc*) tumors, UL49.5-OV therapy reduced untreated, contralateral *sc* tumor size and naturally occurring metastasis. This shows that incorporating a TAP inhibitor into an OV induces both local and systemic antitumor responses following intratumoral administration. Moreover, it establishes arming OVs to evade $CD8^+$ T-cells as an effective OV immunotherapy strategy that may applicable across many OV platforms.

2. Material and Methods

2.1. Cells and Virus Production

All cells were grown and propagated at 37 °C in 5% CO_2 in DMEM plus penicillin (100 U/ml) and streptomycin (0.1 mg/ml), supplemented with the indicated amount of serum [4T1 cells (ATCC CRL-2539) and MBT2 cells (a kind gift from Eva Hernando, NYU School of Medicine): 10% fetal bovine serum (FBS); Vero cells: 5% calf serum; U373 cells: 5% FBS]. To produce HSV-1 stocks for OV therapy, virus was either grown in Vero cells (to treat MBT tumors) or 4T1 cells. Cells were infected (MOI = 0.01 for Vero; MOI = 0.1 for 4T1), incubated at 37 °C, and monitored for the development of cytopathic effects (CPE). After 3 to 4 days, infected cells and supernatant were collected together and frozen at −80 °C. After two freeze thaw cycles, particulate debris was removed by low speed centrifugation (3000 rpm, 5 min, 4 °C). Soluble supernatants containing virus suspensions were recovered, underlaid with a 20% D-Sorbitol cushion in 50 mM Tris–HCl pH 7.2, 1 mM $MgCl_2$ in Ultra-clear centrifuge tubes (*Beckman Coulter*, #344058), and centrifuged at 18,000 rpm [SW-28 Beckman rotor in Optima L-90 k ultra-centrifuge], for 90 min at 4 °C. Pelleted viruses were suspended in 0.5 ml cold PBS and stored at −80 °C. The amount of infectious virus was quantified by plaque assay on Vero cells. A mock preparation isolated in an identical manner from uninfected 4T1 cells was used as a control.

2.2. Mouse In Vivo Models

All animal procedures were performed in accordance with protocols approved by the institutional animal care & use committee at NYU School of Medicine and Noble Life Sciences (Gaithersburg, MD), the animal facility used by BeneVir Biopharm. ARRIVE (Animal Research: Reporting of *In Vivo* Experiments) guidelines (Kilkenny et al., 2010) were followed.

2.2.1. MBT2 Bladder Cancer Model

MBT2 cells (5×10^5) in DPBS (Cellgro, USA) were injected sc into the left and right flanks of 5–6 week old, female C3H/HeN (MBT2) mice anesthetized by continuous inhalation of isoflurane (3% Isoflurane; 1 l/min Oxygen). Tumor growth was monitored using an electronic digital caliper (*VWR International*, *model* # 62379–531). Volume was estimated using the tumor volume formula ($width^2 \times length / 2$). Approximately 10 days post tumor cell inoculation, when tumors reached approximately 50 mm^3, the left flank tumor was directly injected with virus or PBS. Injections were performed on days 0, 3 and 6 with 3×10^5 pfu of BV49.5, BV49.5-FS or PBS. Tumor size (treated left-flank and untreated, contralateral right flank) was monitored over time and animals were euthanized when control-treated tumors reached 1000 mm^3. Prior to MBT2 implantation, mice were immunized as described (Chahlavi et al., 1999) where indicated with 10^5 pfu of wild-type HSV-1 (*Patton strain*) by intraperitoneal injection and boosted with a second injection at the same dose three weeks later. Vaccinated mice were HSV-1 seropositive by immunoblotting.

To determine if UL49.5 promotes persistence of BV49.5 in tumors, C3H/HeN mice with bilateral s.c. MBT-2 tumors were injected over 5 days with three doses of either BV49.5 or BV49.5-FS. Two days after the final injection, mice were sacrificed and tumors were weighed, minced, homogenized using Lysing Matrix D tubes (*MP Biomedical*) and bead-beating, freeze–thawed three times, sonicated and viral titers determined by plaque assay on Vero cells.

2.2.2. 4T1 Breast Cancer Model

4T1 cells (1×10^4) in DMEM without additives were injected sc into the right flank of 8 week old, female *BALB/c* mice anesthetized by ip injection of Ketamine (100 mg/Kg) and Xylazine (10 mg/Kg). Tumor growth was monitored every day using an electronic digital caliper and tumor volume calculated as described (Demaria et al., 2005). When tumors reached approximately 50 mm^3 (8–9 days after 4T1 inoculation), they were directly injected on days 0, 3 and 6 with 10^6 pfu of BV49.5, BV49.5-*FS* or an equivalent virus-free control preparation from uninfected cells. Lung metastasis reportedly occur rapidly, prior to the onset of OV therapy, as clonogenic 4T1 cells were detected by day 7 (Aslakson and Miller, 1992). Tumor size was monitored over time and animals were euthanized when control-treated tumors reached approximately 1200 mm^3. To deplete $CD8^+$ T-cells, 100 μg anti-$CD8^+$ antibody in PBS (*anti-mouse CD8a clone 2.43*, *BioXCell*, *cat.*#BE0061) was injected into each mouse (once daily beginning

3 days prior to commencing OV treatment, and every 6 days thereafter). After 32 days, lungs were isolated and immersed in PFA 4% for one week before superficial lung metastases were quantified by counting under a light microscope. To verify the $CD8^+$ T cell depletion, blood was collected by cardiac puncture using a heparinized syringe and blood cells washed and suspended in RBC lysis buffer (*eBioscience*, *cat.*# 4333–57) to eliminate erythrocytes. After a second wash, cells were stained with anti-mouse CD3, anti-mouse CD4 and a non cross-reactive anti-mouse CD8 monoclonal antibodies (*eBioscience*, *cat.* 11–0032-82, 11–0041-82 and 12–0081-83). Finally, cells were washed and suspended in 4% PFA for FACS analysis.

2.3. Virus Construction

Recombinant HSV-1 Patton strain derivatives were all isolated by homologous recombination of targeting plasmids with viral genomes following co-transfection of viral DNA and plasmid DNA into permissive Vero cells as described (Goins et al., 2002). To create a targeting plasmid capable of introducing an IE-Us11 expression cassette into both $\gamma_1$34.5 loci, the plasmid pSP-Δ34.5-flα27P-Us11-PacI was engineered. This plasmid lacks $\gamma_1$34.5 coding sequences and instead expresses Us11 from the HSV-1 IE ICP27 promoter. It also contains a unique PacI restriction site that can accept a BlpI/PacI fragment containing BHV-1 UL49.5 (WT and *FS*) coding sequences fused to the HCMV promoter. Us11 and UL49.5 coding sequences are surrounded by HSV-1 sequences that normally flank the $\gamma_1$34.5 genes and direct homologous recombination to the Bam HI SP fragment within the viral genome.

To obtain a viral DNA preparation suitable for recombinant virus construction, Vero cells were infected with a $\gamma_1$34.5-deficient (Δ34.5) virus (MOI = 1.0) and the infection was allowed to proceed at 37 °C until cytopathic effect (CPE) was complete. Cells were harvested by low speed centrifugation, suspended in lysate buffer (10 mM EDTA, 10 mM Tris–HCl pH 8.0, 0.6% SDS, 0.25 mg/ml Proteinase K) and agitated overnight at 37 °C. Following phenol/chloroform extraction, approximately 0.2 ml of the aqueous phase was added to 10 ml ethanol. Visible, total DNA (comprised of a mixture of HSV-1 and cellular DNA) was collected by spooling using a sterile glass Pasteur pipette. Excess ethanol was allowed to drain before suspending the DNA in sterile water. The concentration of viral DNA was estimated by plaque assay following transfection into Vero cells.

Targeting plasmid DNA (1 μg) was mixed with DNA isolated from Δ34.5 virus-infected cells (~5 μg) and co-transfected into Vero cells using $CaPO_4$. Once plaques were visible, cell free lysates were prepared by freeze–thawing and 0.1 ml of a ten-fold dilution used to infect non-permissive U373 cells. As Δ34.5 viruses replicate poorly in U373 cells, this step enriches the population for recombinants that express IE Us11 (Mohr and Gluzman, 1996; Mulvey et al., 1999). After three sequential passages in U373 cells, individual isolates were purified three times by limiting dilution in permissive Vero cells. Stocks were prepared of purified isolates in Vero cells and screened for expression of BHV-1 UL49.5 by immunoblotting. The physical genome structure of the recombinants was verified by Southern analysis.

2.4. Antibodies

Antibodies were obtained from the following vendors/individuals: Monoclonal anti-α-Tubulin antibody (*Sigma-Aldrich*, T5168); anti-HSV1 ICP0 antibody [5H7] (*Abcam*, #6513); anti-UL49.5 sera was a kind gift from Geoff Letchworth (Univ. Wyoming) and Emmanuel Wiertz (Univ. Utrecht).

2.5. MHC-I Downregulation Assay

Subconfluent 4T1 cells mock-infected or infected (MOI = 20) with BV49.5 or BV49.5-*FS* were collected by gentle pipetting at 12 hpi. Cell pellets were washed with cold PBS and stained separately for both MHC-1 alleles expressed by BALB/c mice; PE anti-mouse $H\text{-}2D^d$ (#110607, *BioLegend*) and PE anti-mouse $H\text{-}2K^d$ (#116607, *BioLegend*). Isotype control is PE mouse IgG2a, κ (#400211, *Biolegend*). After a 30 min incubation at 4 °C, cells were washed twice with cold PBS, fixed in 4% PFA, and subjected to flow cytometric analysis. Samples were acquired using a LSRII flow cytometer (*BD Biosciences*) and analyzed using FlowJo version 8.8.3.

2.6. IFNγ Production by MBT-2 Stimulated $CD8^+$ Enriched Splenocytes

Spleens were harvested according to IACUC guidelines. Splenocytes were obtained by passing the spleens through a 70 μm mesh, washed with HBSS, and red blood cells were removed with ACK lysis buffer (*Gibco*; *cat.*# A10492-01). Splenocytes were further subjected, following manufacturer's protocol, to a negative selection process to isolate $CD8^+$ T-cells (*Miltenyi Biotec*, *cat.*# 130–095-236). The IFNγ ELISPOT assay was performed as described in the manufacturer's protocol (*eBioscience*, *cat.*# 88–7384). Briefly, the capture antibody was diluted in coating buffer, and 100 μl per well were added into 96-well nitrocellulose plates (*Millipore Corp.*, *cat.*# MAIPS4510). Plates were incubated overnight at 4 °C and thereafter; unbound antibodies were washed away with wash buffer (1 × PBS/0.05% Tween-20). One hundred microliters (μL) of media alone or of mitomycin C-treated (100 μg/ml) MBT2 cells (1×10^5) and 100 μl of the separated CD8 + cells (1×10^5) were added to each well and the plates were incubated for 48 h at 37 °C/5%CO_2. The cells were washed away and 100 μl of biotinylated detection antibody were added and incubated for two hours at RT. Thereafter, the plates were washed and incubated for 45 min at RT with 100 μl Avidin-HRP antibody. Unbound conjugate was removed by another series of washings and finally 100 μl of AEC substrate solution (*Sigma-Aldrich*, *cat.*# A6926) were added, incubated at RT and monitored for the detection of spots. Spots were counted by eye using a dissecting microscope.

2.7. Statistical Analysis

All statistical analysis was carried out using GraphPad Prism 6.0 Software. Significance between treated groups was determined by analysis of variance (ANOVA) followed by post-hoc analysis. Multiple t-test (one unpaired t-test per time point) were also used to establish significance when required. For all analysis, $^*P < 0.05$, $^{**}P < 0.01$, $^{***}P < 0.005$, $^{****}P < 0.001$.

3. Results

To produce a neuroattenuated HSV-1 OV that effectively replicates in tumors and blocks cytosolic peptide display by MHC-I on the surface of infected mouse and human cells, a recombinant deleted for both $\gamma_1$34.5 virulence loci (Δ34.5) was engineered to express HSV-1 Us11 as an IE gene and produce the BHV-1 UL49.5 TAP inhibitor (Fig. 1a, BV49.5). Importantly, while Δ34.5 HSV-1 OVs expressing IE-Us11 counter the limited host defenses in cancer cells and preferentially replicate in tumors, replication and spread of $\gamma_1$34.5-deficient HSV-1 is highly restricted in normal cells and tissues by potent, cell-intrinsic antiviral responses that restricts their growth (Chou et al., 1990; Mohr and Gluzman, 1996; Toda et al., 1999; Rampling et al., 2000; Markert et al., 2000; Mohr et al., 2001; Taneja et al., 2001; Todo et al., 2001; Liu et al., 2003; Mulvey et al., 2004; Hu et al., 2006; Harrington et al., 2010; Senzer et al., 2009; Andtbacka et al., 2015). Furthermore, Δ34.5 OVs expressing IE-Us11 are non-pathogenic in rodents and were also shown to be safe in human trials (Mohr et al., 2001; Taneja et al., 2001; Todo et al., 2001; Liu et al., 2003; Hu et al., 2006; Andtbacka et al., 2015). To avoid introducing additional alterations to the Δ34.5 viral genome, a cassette containing UL49.5 and IE-Us11 genes was targeted by homologous recombination to replace loci formerly occupied by $\gamma_1$34.5-encoding genes. Due to a complex mechanism

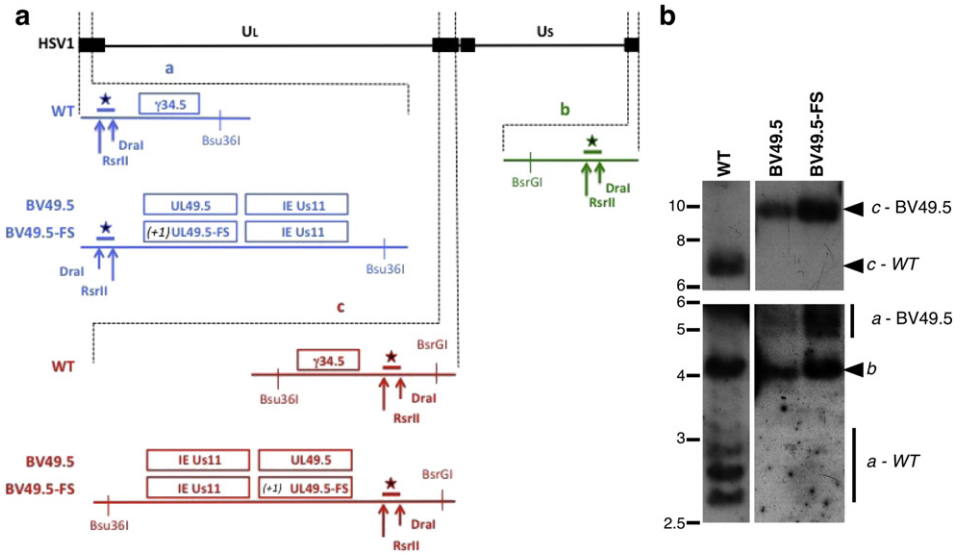

Fig. 1. Physical structure of recombinant HSV-1 OV genomes. a. The linear full-length HSV-1 genome is depicted. Single-copy, unique long (UL) and short (Us) coding segments are shown as solid black lines. Internal and terminal repetitive sequences are shown as filled black rectangles. Regions of the viral genome denoted by dotted lines are expanded below for a detailed view of relevant loci. The γ34.5 gene locus is within a repetitive sequence element and is diploid [*Bsu36I terminal fragment a* (*blue*); *Bsu36I — BsrG1 fragment c* (*red*)]. In the recombinant virus BV49.5, both copies of the γ34.5 gene were replaced with a cassette expressing HSV-1 Us11 as an immediate early (IE) gene and the TAP inhibitor encoded by the bovine herpesvirus 1 UL49.5 gene expressed from the human cytomegalovirus (HCMV) promoter. The recombinant BV49.5-FS is identical to BV49.5 except for a single nucleotide (*indicated as* + 1) that results in a frameshift mutation within the UL49.5 ORF and precludes production of a functional UL49.5 protein. The location of the ^{32}P-labeled DraI-RsrII probe and its three target sites in the genome are depicted as stars (*nucleotides* 48–379 *fragment a*, 125987–126317 *fragment c*, 151910–152241 *fragment b*). b. DNA isolated from virus-infected cells was doubly digested with BsrGI-Bsu36I, fractionated by electrophoresis on a 1% agarose gel, transferred to a nylon membrane and hybridized to the ^{32}P-labeled DraI-RsrII probe (depicted as a star in a.) This probe identifies sequences within internal and terminal repetitive genome segments that lie outside of the γ34.5 ORF. Hybridizing fragments (*a*, *b*, *c delineated in panel a*) from WT, BV49.5, and BV49.5-FS viruses are indicated on the right of the autoradiogram. The mobility of DNA molecular size standards (in Kb) is indicated on the left. Shorter (top panels) and longer (bottom panels) exposures are shown to facilitate visualization of terminal fragments that are underrepresented in replicating concatameric genomes. Intervening lanes between WT, BV49.5, and BV49.5-FS have been spliced out. Heterogeneity at the genomic *Bsu36I* terminal fragments is due to natural variations within a repetitive sequence component.

involving both N and C terminal protein domains, it has not been possible to isolate minimal amino acid substitutions within the UL49.5 ORF that selectively ablate UL49.5 TAP inhibitory activity (Loch et al., 2008; Verweij et al., 2011b; Wei et al., 2011). Instead, an otherwise isogenic variant differing by one additional nucleotide within UL49.5 that results in a frameshift (FS) and is unable to produce functional UL49.5 was constructed (BV49.5-FS). Physical genomic analysis of viral recombinants was performed using stocks grown up following three consecutive limiting dilution steps to purify single plaques. The genome structure was verified by Southern analysis (Fig. 1b) and indicated that the recombinant viruses are genetically stable even after the extensive amplification associated with three sequential plaque purifications and subsequent high-titer stock preparation. Note that while Bsu36I terminal fragments of WT length (Fig. 1b, *fragments marked a-WT*) are readily observed in DNA isolated from WT HSV-1-infected cells, they were not detected in samples from cells infected with BV49.5 or BV49.5-FS. Instead, Bsu36I terminal fragments in BV49.5 or BV49.5-FS migrate slower (Fig. 1b, *fragments marked a-BV49.5*), consistent with their greater length due to inclusion of Us11 and UL49.5 ORFs. Likewise, internal BsrGI-Bsu36I fragments of WT length (Fig. 1b, *fragments marked c-WT*) are only detected in WT virus, but not in samples from cells infected with BV49.5 or BV49.5-FS. Instead, internal BsrGI-Bsu36I fragments in BV49.5 and BV49.5-FS modified to include Us11 and UL49.5 ORFs migrated slower reflecting their larger size (Fig. 1b, *fragments marked c-BV49.5*). As expected, alterations in the length of terminal BsrGI fragments (Fig. 1b, *fragments marked b*) were not detected in WT, BV49.5, or BV49.5-FS viruses. This shows that BV49.5 and BV49.5-FS recombinants contain the expected modified terminal and internal HSV-1 genome fragments capable of encoding IE-Us11 and functional or non-functional UL49.5 variants.

To evaluate the capacity of the newly isolated recombinants to express BHV-1 UL49.5, total protein was isolated from virus-infected cells and analyzed by immunoblotting. BHV UL49.5 protein only accumulated in BV49.5-infected cells and was not detected in cells infected with the BV49.5-FS variant, wild-type (WT) HSV-1, or the parental Δ34.5 mutant (Fig. 2a). Furthermore, cell surface MHC class I was significantly reduced in cells infected with BV49.5 compared to BV49.5-FS (Fig. 2b,c). Finally, BV49.5 and BV49.5-FS replicated to equivalent levels in murine 4T1 breast cancer cells and MBT2 bladder cancer cells (Fig. 2d), demonstrating that the FS variant does not produce a protein that inhibits virus replication in the absence of innate and acquired immune responses. In addition, both BV49.5 and BV49.5-FS replicated better than an ICP34.5-deficient virus because IE-Us11 expression allows Δ34.5 viruses to overcome host innate immune defenses that restrict protein synthesis and limit viral replication (Mohr and Gluzman, 1996; Mulvey et al., 1999; Taneja et al., 2001; Todo et al., 2001).

To evaluate OV therapeutic responses in treated and untreated tumors in the same animal, bilateral *sc* MBT2 tumors were established in the flanks of C3H/HeN mice. Previous studies have shown HSV-1 OV intra-tumoral injection of one tumor induced regression of the treated and untreated, contralateral tumor, while OV was only detected in the treated tumor (Toda et al., 1999). In addition, regression of the uninjected, contralateral tumor was dependent upon an anti-tumor $CD8^+$ T-cell response (Toda et al., 1999). Prior to inoculating with MBT2 cells, mice were vaccinated with HSV-1 according to a published procedure (45) to ensure that mice could rapidly mount an adaptive immune response against HSV-1 following OV administration and model future applicability to the clinic where most patients will have pre-existing immunity to HSV-1. As prior vaccination with HSV-1 was not required to observe differences between viruses expressing a functional vs non-functional UL49.5 gene product in rodents (Figs. 4 and 5, S2 and *unpub. obs.*), subsequent work was performed in mice that were not HSV-1 seropositive prior to the onset of the experiment. Once tumors reached approximately 50 mm^3, each left flank tumor was directly injected with a vehicle control, BV49.5 or BV49.5-FS.

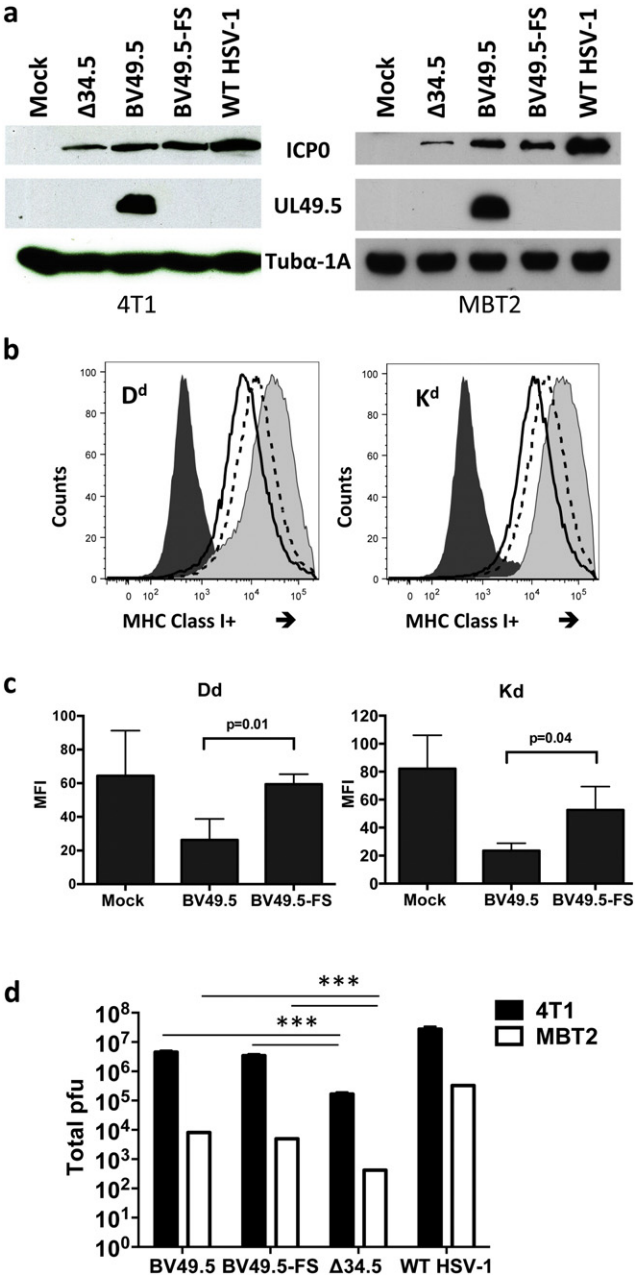

Fig. 2. Developing an HSV-1 OV that evades innate and cell-mediated immune responses. a. Immunoblot analysis of UL49.5 protein accumulation following high multiplicity infection (MOI = 20) of murine bladder (MBT2) and breast (4T1) cancer cell lines with the indicated viruses (18 h post-infection). Antisera specific for HSV-1 ICP0 and tubulin served as controls. b. UL49.5 expression by BV49.5 functions to down-regulate cell surface MHC class I expression in 4T1 cells. Cells were mock-infected (*solid gray curve*) or infected (MOI = 5) with BV49.5 (*solid black line*) or BV49.5-FS (*broken black line*) and subsequently fixed and stained with the indicated antibody. Left panel: anti-MHC-I H2-D^d Ab staining, Right panel: anti-MHC-I H2-K^d Ab staining. Staining of infected cells with non-immune sera is shown by the leftmost solid black curve. c. As in b but bar graphs show MFI after adjusting for background staining of isotype antibody. Data were collected from 3 independent experiments +/− SD. d. BV49.5 and BV49.5-FS replicate equivalently in cultured murine cancer cells. MBT2 (MOI = 0.02) or 4T1 (MOI = 0.5) cells were infected with the indicated virus and after 3 days (4T1) or 4 days (MBT2), the amount of infectious virus present in cell free lysates was quantified by plaque assay in permissive Vero cells. *** $P < 0.005$ by student's t-test.

Additional intra-tumoral injections were performed 3 and 6 d after the first treatment and the volume of treated and untreated, contra-lateral tumors measured over time. While injecting either BV49.5 or BV49.5-FS reduced treated-tumor volume compared to vehicle alone, BV49.5 was significantly more effective over 12 d (Fig. 3a; Supplemental table S1). Furthermore, BV49.5 was more effective treating contra-lateral tumors than BV49.5-FS (Fig. 3b; Table S1). As BV49.5-FS does not express UL49.5 but is otherwise identical to BV49.5, UL49.5 protein expression was likely responsible for the superior treatment outcome.

To further rule out any untoward effects of the FS mutation, BV49.5 anti-tumor activity was compared to three additional HSV-1 Δ34.5 OVs expressing IE-Us11. Instead of UL49.5, BV-mGMCSF expresses mouse GMCSF (mGMCSF) based on earlier studies claiming this improves the activity of Δ34.5 OVs expressing IE-Us11 (Liu et al., 2003) and the recent biologics licensing application approval of a Δ34.5 IE-Us11 HSV-1 OV expressing human GMCSF by the FDA (Dolgin, 2015; http://www.fda.gov/BiologicsBloodVaccines/CellularGeneTherapyProducts/ApprovedProducts/ucm469411.htm). Levels of mGMCSF produced by BV-mGMCSF and detected by ELISA (*unpub. obs*) were similar to those reported for another Δ34.5 IE Us11 expressing virus (Liu et al., 2003). A variant of BV-mGMCSF was engineered that expressed UL49.5 (BV49.5-mGMCSF). The physical structure of these recombinants was verified by Southern analysis and their comparative growth properties in cultured MBT2 cells evaluated (Fig. S1). As an additional control, the first Δ34.5 IE Us11 expressing virus (SUP1) to show efficacy as an HSV-1 OV was included (Taneja et al., 2001). In all cases, UL49.5-expressing OVs were superior in treating directly injected and contra-lateral tumors than viruses unable to express UL49.5 (Fig. S2). Thus, arming an HSV-1 OV with a TAP inhibitor stimulated its anti-tumor activity both in treated primary tumors and in untreated distal tumors. In addition, GMCSF expression did not detectably alter the efficacy of an OV expressing the UL49.5 TAP inhibitor under these conditions (Fig. S2).

To investigate how UL49.5 expression promoted OV anti-tumor activity, we first determined if UL49.5 expression enabled viral persistence in tumors. After establishing bilateral s.c. MBT2 tumors, left flank tumors were treated with BV49.5 or the FS variant as in Fig. 3a. Two days after the final injection, infectious virus load in OV-treated and untreated (contra-lateral) tumors was determined. BV49.5-treated tumors contained on average 7-fold more virus than BV49.5-FS-treated tumors (Fig. 3c) and infectious virus was not detected in untreated, contralateral tumors (*not shown*). Thus, functional UL49.5 protein promotes OV persistence in tumors presumably by inhibiting TAP in infected cells. Greater OV persistence likely supports more tumor cell oncolysis and fuels development of $CD8^+$ T-cells that recognize tumor antigens. To determine if UL49.5 TAP-inhibitor expression influenced development of anti-tumor, cell-mediated immunity, antigen-stimulated IFNγ release by CTL isolated from vehicle or OV-treated mice was evaluated. While IFNγ secretion by $CD8^+$-enriched splenocytes from BV49.5-FS or vehicle-treated mice in response to mitomycin C-treated MBT2 cell stimulation was not detectable, IFNγ release was significantly elevated by approximately 5-fold only in splenocytes isolated from BV49.5-treated mice (Fig. 3d). This finding is consistent with the notion that UL49.5-mediated TAP inhibition promotes anti-tumor immunity.

To investigate if a TAP inhibitor-armed OV was advantageous in treating other solid tumors, a mouse mammary cancer model was tested (4T1). This well-characterized model allows primary tumor measurements after direct OV delivery and reliably produces readily quantifiable lung metastases, obviating the need to implant tumors at a distant site and allowing us to take advantage of the more physiologically relevant, natural capacity of murine 4T1 breast cancer cells to metastasize to the lung. Moreover, therapy-induced regression of metastatic tumors is dependent on $CD8^+$ T-cell responses (Demaria et al., 2005). Fig. 4a shows that BV49.5 was more effective than BV49.5-FS at treating primary 4T1 *sc* tumors. The enhanced anti-tumor activity of BV49.5 vs BV49.5-FS was significant by 13 d after treatment and improved over time (Fig. 4a; table S2). To determine if the efficacy of BV49.5 compared to the FS variant was due to therapy-induced anti-tumor $CD8^+$ T-cells, OV treatment was evaluated in CD8 + T-cell-depleted mice. Significantly, the greater efficacy of BV49.5 over BV49.5-FS was abrogated by $CD8^+$ T-cell depletion

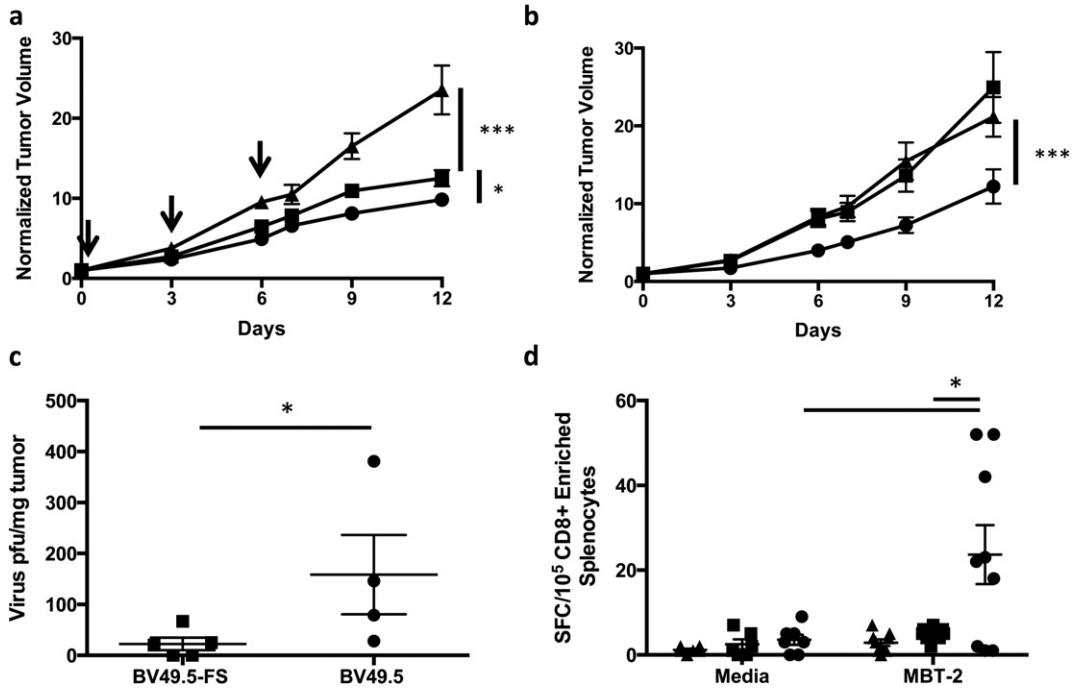

Fig. 3. Stimulation of anti-tumor activity at local and distant sites by arming an OV with a TAP inhibitor. a. Bilateral, sc MBT2 tumors were established in left and right flanks of C3H/HeN mice that were vaccinated previously with HSV-1. Left flank tumors were treated on the indicated days (arrows) by intratumoral injection of BV49.5 (●; n = 24), BV49.5-FS (■; n = 23), or PBS (▲; n = 20). Tumors were measured on the indicated days and the average normalized values reflecting relative tumor size on each day were plotted. Initial tumor volume immediately before treatment was normalized to a relative size of 1.0. Error bars reflect the SEM. Control-treated tumors were compared to BV49.5 and BV49.5-FS-treated tumors by two-way ANOVA followed by Tukey's post-hoc analysis (****P value < 0.001). b. As in (a) except contralateral (right flank), untreated tumors were plotted. ***P value <0.005 by Two-Way ANOVA. c. After 2 d, tumors were harvested from mice that were not vaccinated and the amount of infectious virus present in cell free lysates quantified by plaque assay in Vero cells. *P value < 0.05 by student's t-test. d. IFNγ production by splenocytes isolated from mice treated as in (a) and stimulated with either media or mitomycin c-treated MBT2 cells. Splenocytes were isolated on day 10 or ten days after the first virus treatment. *P value < 0.05 by student's t-test.

(Fig. 4b,c; table S2). Thus, the superior therapeutic activity of BV49.5 was dependent upon: 1) a single nucleotide difference from BV49.5-FS that enabled TAP inhibitor production; and 2) a host $CD8^+$ T-cell response. Remarkably, BV49.5 was likewise more effective than BV49.5-FS in reducing the number of lung metastases, whereas BV49.5-FS was not detectably better than treatment with vehicle alone (Fig. 5a,b). Significant differences in the number of lung metastases were not detected in BV49.5 vs BV49.5-FS vs vehicle alone-treated mice following $CD8^+$-depletion of BV49.5-treated animals (Fig. 5c). Similar to our findings treating primary 4T1 tumors, the superiority of BV49.5 in reducing lung metastases compared to BV49.5-FS was dependent upon production of the UL49.5 TAP inhibitor and intact $CD8^+$ T-cell responses. Thus, therapy of primary tumors with a TAP inhibitor-armed OV effectively treated tumors at distant sites in two different models, one using a preformed tumor at a contralateral site (MBT2) and another that undergoes more physiological dissemination via natural metastases (4T1).

4. Discussion

By restricting OV replication and spread, host $CD8^+$ T cell responses limit direct tumor oncolysis and the development of a systemic anti-tumor response.

Although many herpesviruses, including HSV-1, encode a TAP inhibitor to evade $CD8^+$ T-cells and productively replicate in the presence of $CD8^+$ T-cells, the gene encoding the HSV-1 TAP inhibitor ICP47 has been deleted in many OVs (Taneja et al., 2001; Todo et al., 2001; Liu et al., 2003; Hu et al., 2006; Senzer et al., 2009; Harrington et al., 2010; Andtbacka et al., 2015). Since ICP47 is species specific and not functional in rodents (Ahn et al., 1996; Tomazin et al., 1996), its importance previously went unnoticed in preclinical studies. Furthermore, while removing ICP47 has been widely assumed to benefit OV immunotherapy, a direct comparison of how TAP inhibitor expression might impact OV therapeutic efficacy was not previously performed in a responsive model (Lichty et al., 2014). By engineering an HSV-1 OV expressing the BHV-1 UL49.5 TAP inhibitor, which functions in rodent preclinical models and humans (Verweij et al., 2011a), we show that this OV produces superior therapeutic outcomes compared to three independently isolated OVs unable to produce UL49.5. Not only is a UL49.5-expressing OV a more effective anti-tumor agent following local administration into primary tumors, it is also more potent at reducing tumor growth at distant, untreated sites in two different murine solid tumor cancer models. Moreover, the benefit of UL49.5 expression on OV therapeutic efficacy is dependent upon $CD8^+$ T-cells, which may confer long-lived protection. This establishes inhibiting TAP in infected tumor cells as an effective mechanism to promote OV immunotherapeutic action.

While precisely how TAP inhibitors like UL49.5 augment OV therapy and promote $CD8^+$-dependent anti-tumor immune responses are unknown, evading CTLs is likely important. By shielding infected cells from elimination, TAP inhibitor armed OVs persist longer (Fig. 2c). Importantly, BV49.5 was not detectably more pathogenic than BV49.5 and *never* spread to contralateral, untreated tumors despite replicating to greater levels in directly-injected, treated tumors. Furthermore, no adverse effects associated with HSV-1 pathogenesis and virulence were observed throughout this study in any of the treated mice, even after multiple injections and upon CD8 + T cell depletion. This is consistent with OV replication being limited to the treated tumor and restricted OV growth and spread in normal tissue as has been reported for numerous HSV-1 Δ34.5 OVs (Rampling et al., 2000; Markert et al., 2000; Taneja et al., 2001; Todo et al., 2001; Hu et al., 2006; Senzer et al., 2009; Harrington et al., 2010; Andtbacka et al., 2015). Longer OV persistence within tumors could cause greater oncolysis in the primary tumor despite preexisting antiviral immunity. This likely generates more tumor associated antigens (TAA) available for cross-presentation by dendritic cells (DCs) to anti-tumor $CD8^+$ CTL. Significantly, downregulating antigen presentation and evading

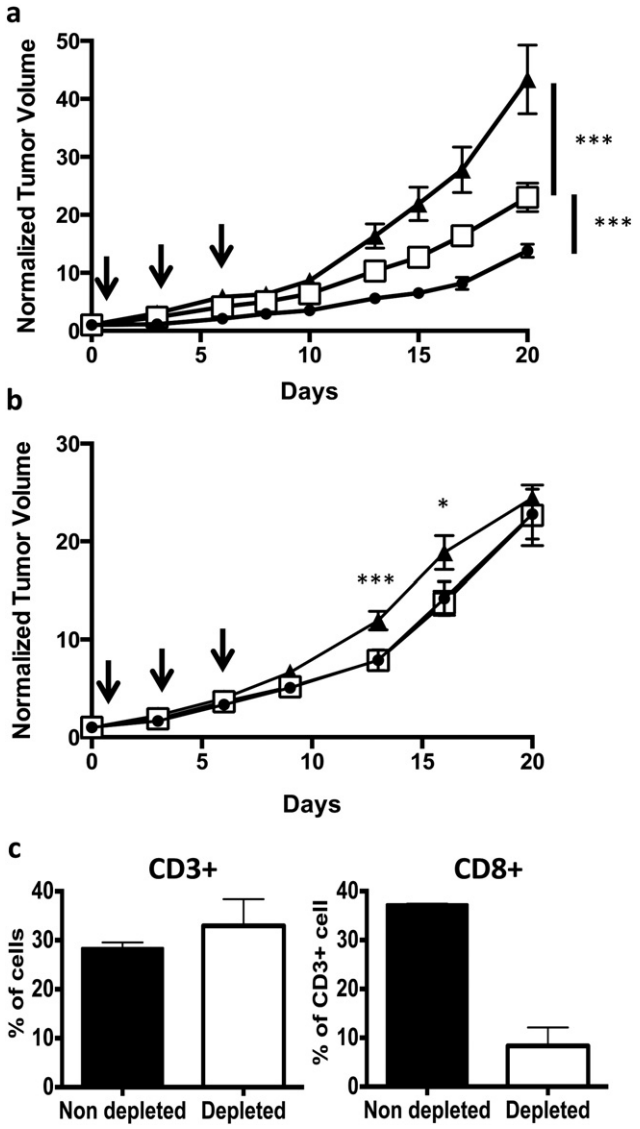

Fig. 4. CD8$^+$ T cell-dependent anti-tumor responses induced by treatment with an OV armed with a TAP-inhibitor. a. Mouse mammary sc tumors (4T1) in BALB/c mice were treated on the indicated days (arrows) by intratumoral injection of BV49.5 (●; n = 9), BV49.5-FS (□; n = 10), or PBS (▲; n = 10). Tumors were measured on the indicated days and the average normalized values reflecting relative tumor size on each day were plotted. Initial tumor volume immediately before treatment was normalized to a relative size of 1.0. Control-treated tumors were compared to BV49.5 and BV49.5-FS-treated tumors by two-way ANOVA followed by Tukey's post-hoc analysis (****P value < 0.001). b. As in (a) except mice (n = 10) were injected with anti-CD8$^+$ antibody to selectively deplete CD8$^+$ T-cells. *P < 0.05; ***P < 0.005 by student's t-test. c. Splenic T-cell populations before (*non-depleted*) and after (*depleted*) CD8$^+$ T-cell depletion were analyzed by FACS using anti-CD3 and anti-CD8 antibody. Error bars reflect SEM.

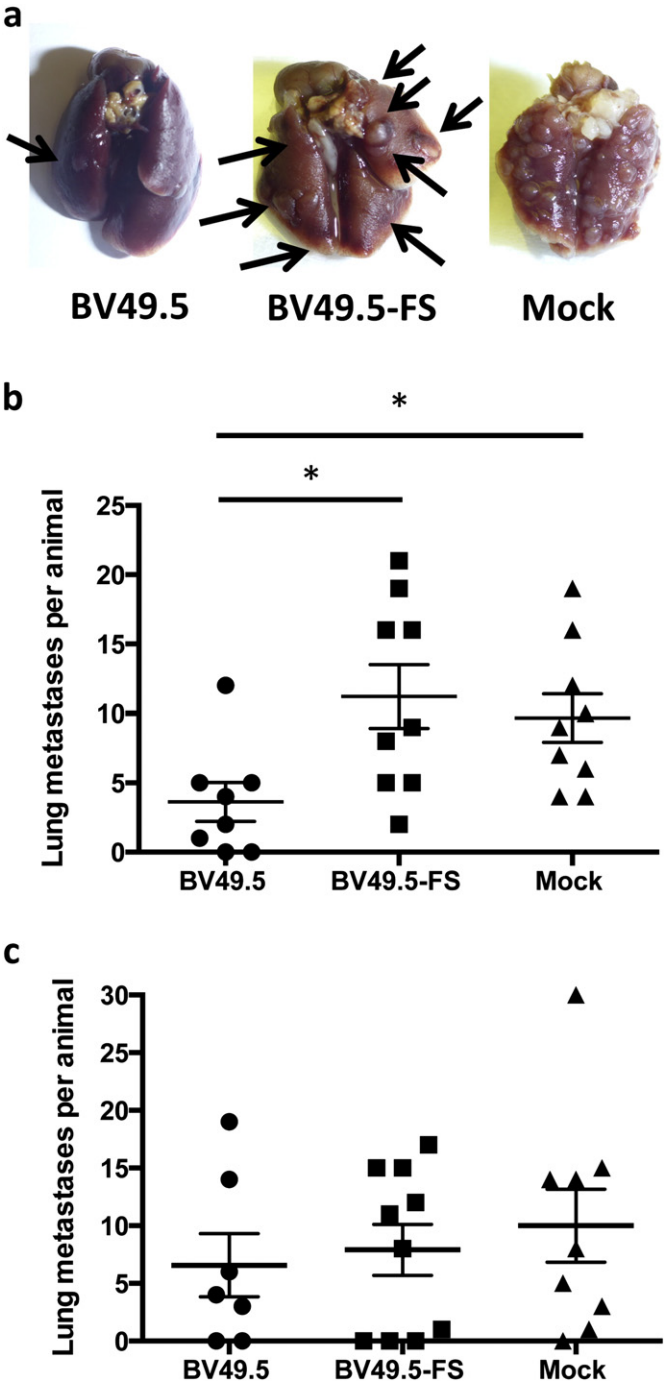

Fig. 5. Reduced lung metastasis induced by immunotherapy with a TAP-inhibitor-armed OV. BALB/c mice with mouse mammary sc tumors (4T1) were treated on d 1, 3 and 6 as in Fig. 4. Mice were sacrificed 26 d after the initiation of treatment and lungs were fixed in formalin. a. Representative lungs showing metastases (arrows) in mice from a treated with BV49.5, BV49.5-FS, or PBS. b. The number of lung metastases was quantified by counting under a light microscope. c. Lung metastases were quantified in mice injected with anti-CD8 antibody to selectively deplete CD8$^+$ T-cells as in Fig. 4b. P < 0.005***; P < 0.05* using Mann–Whitney statistics.

anti-viral CD8$^+$ CTLs by a TAP inhibitor-armed OV resembles a mechanism used by some advanced tumors to evade elimination by anti-tumor CTL (Leone et al., 2013). Although TAA display is reduced in tumors with antigen presentation defects, antigen presentation is not eliminated so long as peptides are processed and access MHC class I via a TAP-independent manner. Indeed, TAP-deficient tumors instead display an MHC class I - peptide antigen repertoire derived from alternative sources, including signal peptides generated by co-translational cleavage in the ER lumen or peptides generated in other compartments (trans Golgi, endosomal) that subsequently enter the ER (*reviewed in* Oliveira and van Hall, 2013). Display of an alternate peptide repertoire in TAP-inhibited cells, including those ectopically expressing BHV-1 UL49.5, reportedly contributes to immune recognition of TAP-inhibited cells by CD8$^+$ T-cells (Lampen et al., 2010). Perhaps remodeling MHC class I — peptide antigen repertoires following TAP-inhibitor armed OV treatment might in part influence immunotherapeutic, anti-tumor responses (van Hall et al., 2006).

Our findings are also consistent with results showing that evading T-cell responses is critical for superinfecting monkeys previously colonized by the related herpesvirus cytomegalovirus (Hansen et al.,

2010), as HSV-1 OV treatment of HSV-1 positive subjects and initially HSV-1 negative patients that seroconvert after the first dose can be considered a form of superinfection. Furthermore, they support a model where an OV expressing the UL49.5 TAP inhibitor to evade $CD8^+$ CTLs exerts both local and global effects, facilitating viral replication and direct oncolysis within a tumor thus stimulating a global anti-tumor immune response. Finally, they establish that the systemically-acting, immunotherapeutic power of local OV administration is effectively enabled by harnessing the natural ability of HSV to persist in the face of $CD8^+$ T-cell responses. TAP-inhibitor armed OVs might better synergize with immune checkpoint inhibitors (Zamarin et al., 2014), or possibly be sufficiently potent as single agents compared to OVs unable to inhibit TAP.

5. Conclusions

Oncolytic viruses (OVs) offer advantages over traditional cancer therapies by selectively killing tumor cells and stimulating anti-tumor immune responses. However, vulnerability to CD8 + T-cell clearance limits therapeutic responses to OVs. Using a herpes simplex virus-1 OV model, we engineer an OV that evades $CD8^+$ T-cells by expressing a herpesvirus-encoded inhibitor of TAP (*transporter associated with antigen processing*). Our results show OVs that inhibit TAP demonstrate greater efficacy treating bladder and breast cancer in a manner dependent upon CD8 + T-cell immune responses in pre-clinical mouse models. Moreover, they were better able to stimulate systemic anti-tumor responses that reduced distant, untreated tumors and natural metastases. This establishes that arming OVs to evade $CD8^+$ T cells as an effective OV immunotherapy strategy.

Funding Sources

This work was supported by an Applied Research Support Fund Award from the NYU Office of Industrial Liaison, center of excellence funding from NYU School of Medicine to the Dept of Urology, and a translational pilot project award from the NYU Cancer Institute center grant from NIH (5P30CA016087) to IM. IM was also supported in part by NIH Grants AI073898 and GM056927. AP was supported in part by funds from the Philippe Foundation. SD was supported by grants from the USA Department of Defense (DOD) Breast Cancer Research Program (BCRP) (W81XWH-11-1-0532), and The Chemotherapy Foundation. ABF was supported by NIH grant R01 CA108573. Work at Benevir was supported in part by NCI SBIR Phase 1 grant 1R43CA168172-01A1. External funding sources did not have any involvement with study design, data collection, data interpretation, preparing the manuscript or the decision to submit the manuscript for publication.

Conflict of Interest Statement

SRF and MM are employees of Benevir Biopharm and hold stock and/or options in the company. AP, ABF, and IM consult for Benevir Biopharm and hold stock and/or options in the company. The remaining authors have no competing interests to declare.

Author Contributions

AP, SRF, and KAP performed and designed experiments, analyzed data, and assisted writing the manuscript. ABF and SD designed experiments, analyzed data and assisted writing the manuscript. IM and MM designed experiments, analyzed the data, and wrote the manuscript.

Acknowledgments

We thank members of the Mohr lab for many helpful discussions and are grateful to Michael Garabedian, Herb Lepor, and Xue Ru-Wu for support from the Dept. of Urology Center of Excellence.

Appendix A. Supplementary data

Supplementary data to this article can be found online at http://dx.doi.org/10.1016/j.ebiom.2016.01.022.

References

Ahn, K., et al., 1996. Molecular mechanism and species specificity of TAP inhibition by herpes simplex virus ICP47. EMBO J. 15, 3247–3255.
Altomonte, J., et al., 2009. Enhanced oncolytic potency of vesicular stomatitis virus through vector-mediated inhibition of NK and NKT cells. Cancer Gene Ther. 16, 266–278.
Andtbacka, R.H., et al., 2015. Talimogene laherparepvec improves durable response rate in patients with advanced melanoma. J. Clin. Oncol. 33, 2780–2788.
Aslakson, C.J., Miller, F.R., 1992. Selective events in the metastatic process defined by analysis of the sequential dissemination of subpopulations of a mouse mammary tumor. Cancer Res. 52, 1399–1405.
Bell, J., McFadden, G., 2014. Viruses for tumor therapy. Cell Host Microbe 15, 260–265.
Brown, M.C., et al., 2014. Oncolytic polio virotherapy of cancer. Cancer http://dx.doi.org/10.1002/cncr.28862.
Chahlavi, A., Rabkin, S.D., Todo, T., Sundaresan, P., Martuza, R.L., 1999. Effect of prior exposure to herpes simplex virus 1 on viral vector-mediated tumor therapy in immunocompetent mice. Gene Ther. 6, 1751–1758.
Chiocca, E.A., Rabkin, S.B., 2014. Oncolytic viruses and their application to cancer immunotherapy. Cancer Immunol. Res. 2, 295–300.
Chou, J., Kern, E.R., Whitley, R.J., Roizman, B., 1990. Mapping of herpes simplex virus-1 neurovirulence to gamma (1) 34.5, a gene nonessential for growth in culture. Science 250, 1262–1266.
Demaria, S., et al., 2005. Immune-mediated inhibition of metastases after treatment with local radiation and ctla-4 blockade in a mouse model of breast cancer. Clin. Cancer Res. 11, 728–734.
Dharmadhikari, N., Mehnert, J.M., Kaufman, H.L., 2015. Oncolytic virus immunotherapy for melanoma. Curr. Treat. Options in Oncol. 16 (3), 326.
Dolgin, E., 2015. Oncolytic viruses get a boost with first FDA-approval recommendation. Nat. Rev. Drug Discov. 14, 369–371.
Früh, K., et al., 1995. A viral inhibitor of peptide transporters for antigen presentation. Nature 375, 415–418.
Fulci, G., et al., 2006. Cyclophosphamide enhances glioma virotherapy by inhibiting innate immune responses. Proc. Natl. Acad. Sci. U. S. A. 103, 12873–12878.
Goins, W.F., et al., 2002. Construction of replication-defective herpes simplex virus vectors. Curr. Protoc. Hum. Genet. 12.11.1–12.11.30.
Hansen, S.G., et al., 2010. Evasion of $CD8^+$ T cells is critical for superinfection by cytomegalovirus. Science 328, 102–106.
Haralambieva, I., et al., 2007. Engineering oncolytic measles virus to circum-vent the intracellular innate immune response. Mol. Ther. 15, 588–597.
Harrington, K.J., et al., 2010. Phase I/II study of oncolytic HSV GM-CSF in combination with radiotherapy and cisplatin in untreated stage III/IV squamous cell cancer of the head and neck. Clin. Cancer Res. 16, 4005–4015.
He, B., et al., 1997. Suppression of the phenotype of 134.5 herpes simplex virus type 1: Failure of activated RNA-dependent protein kinase to Shut off protein synthesis is associated with a deletion in the domain of the 47 gene. J. Virol. 71, 6049–6054.
Hill, A., et al., 1995. Herpes simplex virus turns off the TAP to evade host immunity. Nature 375, 411–415.
Hu, J.C., et al., 2006. A phase I study of OncoVEXGM-CSF, a second-generation oncolytic herpes simplex virus expressing granulocyte macrophage colony-stimulating factor. Clin. Cancer Res. 12, 6737–6747.
Ikeda, K., et al., 1999. Oncolytic virus therapy of multiple tumors in the brain requires suppression of innate and elicited antiviral responses. Nat. Med. 5, 881–887.
Kaufman, H.L., Kohlhapp, F.J., Zloza, A., 2015. Oncolytic viruses: a new class of immunotherapeutic drugs. Nat. Rev. Drug Discov. 14, 642–662.
Kilkenny, C., Browne, W.J., Cuthill, I.C., Emerson, M., Altman, D.G., 2010. Improving bioscience research reporting: the ARRIVE guidelines for reporting animal research. PLoS Biol. 8 (6), e1000412.
Koelle, D.M., et al., 1993. Herpes simplex virus infection of human fibroblasts and keratinocytes inhibits recognition by cloned CD8 + cytotoxic T lymphocytes. J. Clin. Invest. 91, 961–968.
Koppers-Lalic, D., et al., 2005. Varicelloviruses avoid T cell recognition by UL49.5-mediated inactivation of the transporter associated with antigen processing. Proc. Natl. Acad. Sci. U. S. A. 102, 5144–5149.
Lampen, M.H., et al., 2010. $CD8^+$ T cell responses against TAP-inhibited cells are readily detected in the human population. J. Immunol. 185, 6508–6517.
Le Bœuf, F., et al., 2013. Model-based rational design of an oncolytic virus with improved therapeutic Potential. Nat. Commun. 4, 1974.
Leone, P., et al., 2013. MHC class I antigen processing and presenting machinery: organization, function, and defects in tumor cells. J. Natl. Cancer Inst. 105, 1172–1187.
Lichty, B.D., Breitbach, C.J., Stojdl, D.F., Bell, J.C., 2014. Going viral with cancer immunotherapy. Nat. Rev. Cancer 14, 559–567.
Liu, B.L., et al., 2003. ICP34.5 deleted herpes simplex virus with enhanced oncolytic, immune stimulating, and anti-tumour properties. Gene Ther. 10, 292–303.
Liu, T.-C., Galanis, E., Kirn, D., 2007. Clinical trial results with oncolytic virotherapy: a century of promise, a decade of progress. Nat. Clin. Pract. Oncol. 4, 101–117.
Loch, S., Klauschies, F., Schölz, C., Verweij, M.C., Wiertz, E.J., Koch, J., Tampé, R., 2008. Signaling of a varicelloviral factor across the endoplasmic reticulum membrane

induces destruction of the peptide-loading complex and immune evasion. J. Biol. Chem. 283, 13428–13436.
Markert, J.M., et al., 2000. Conditionally replicating herpes simplex virus mutant, G207 for the treatment of malignant glioma: results of a phase I trial. Gene Ther. 7, 867–874.
Mohr, I., Gluzman, Y., 1996. A herpesvirus genetic element which affects translation in the absence of the viral GADD34 function. EMBO J. 15, 4759–4766.
Mohr, I., et al., 2001. A herpes simplex virus type 1 gamma34.5 second-site suppressor mutant that exhibits enhanced growth in cultured glioblastoma cells is severely attenuated in animals. J. Virol. 75, 5189–5196.
Mulvey, M., Poppers, J., Ladd, A., Mohr, I., 1999. A herpesvirus ribosome-associated, RNA-binding protein confers a growth advantage upon mutants deficient in a GADD34-related function. J. Virol. 73, 3375–3385.
Mulvey, M., Camarena, V., Mohr, I., 2004. Full resistance of herpes simplex virus type 1-infected primary human cells to alpha interferon requires both the Us11 and gamma(1)34.5 gene products. J. Virol. 78, 10193–10196.
Nguyên, T.L., et al., 2008. Chemical targeting of the innate antiviral response by histone deacetylase inhibitors renders refractory cancers sensitive to viral oncolysis. Proc. Natl. Acad. Sci. U. S. A. 105, 14981–14986.
Oliveira, C.C., van Hall, T., 2013. Importance of TAP-independent processing pathways. Mol. Immunol. 55, 113–116.
Posvad, C.M., Rosenthal, K.L., 1992. Herpes simplex virus-infected human fibroblasts are resistant to and inhibit cytotoxic T-lymphocyte activity. J. Virol. 66, 6264–6272.
Rampling, R., et al., 2000. Toxicity evaluation of replication-competent herpes simplex virus (ICP 34.5 null mutant 1716) in patients with recurrent malignant glioma. Gene Ther. 7, 859–866.
Senzer, N.N., et al., 2009. Phase II clinical trial of a granulocyte-macrophage colony-stimulating factor–encoding, second-generation oncolytic herpesvirus in patients with unresectable metastatic melanoma. J. Clin. Oncol. 27, 5763–5771.
Taneja, S., MacGregor, J., Markus, S., Ha, S., Mohr, I., 2001. Enhanced antitumor efficacy of a herpes simplex virus mutant isolated by genetic selection in cancer cells. Proc. Natl. Acad. Sci. U. S. A. 98, 8804–8808.
Toda, M., Rabkin, S.D., Kojima, H., Martuza, R.L., 1999. Herpes simplex virus as an in situ cancer vaccine for the induction of specific anti-tumor immunity. Hum. Gene Ther. 10, 385–393.
Todo, T., Martuza, R.L., Rabkin, S.D., Johnson, P.A., 2001. Oncolytic herpes simplex virus vector with enhanced MHC class I presentation and tumor cell killing. Proc. Natl. Acad. Sci. U. S. A. 98, 6396–6401.
Tomazin, R., et al., 1996. Stable binding of the herpes simplex virus ICP47 protein to the peptide binding site of TAP. EMBO J. 15, 3256–3266.
van Hall, T., et al., 2006. Selective cytotoxic T-lymphocyte targeting of tumor immune escape variants. Nat. Med. 12, 417–424.
Verweij, M.C., et al., 2011a. Inhibition of mouse TAP by immune evasion molecules encoded by non-murine herpesviruses. Mol. Immunol. 48, 835–845.
Verweij, M.C., et al., 2011b. Structural and functional analysis of the TAP-inhibiting UL49.5 proteins of varicelloviruses. Mol. Immunol. 48, 2038–2051.
Wang, Y., et al., 2003. E3 gene manipulations affect oncolytic adenovirus activity in immunocompetent tumor models. Nat. Biotechnol. 21, 1328–1335.
Wei, H., Wang, Y., Chowdhury, S.I., 2011. Bovine herpesvirus type 1 (BHV-1) UL49.5 luminal domain residues 30 to 32 are critical for MHC-I down-regulation in virus-infected cells. PLoS One 6, e25742.
York, I., et al., 1994. A cytosolic herpes simplex virus protein inhibits antigen presentation to CD8+ T lymphocytes. Cell 77, 525–535.
Zamarin, D., et al., 2009. Enhancement of oncolytic properties of recombinant Newcastle disease virus through antagonism of cellular innate immune responses. Mol. Ther. 17, 697–706.
Zamarin, D., Holmgaard, R.B., Subudhi, S.K., Park, J.S., Mansour, M., Palese, P., Merghoub, T., Wolchok, J.D., Allison, J.P., 2014. Localized oncolytic virotherapy overcomes systemic tumor resistance to immune checkpoint blockade immunotherapy. Sci. Transl. Med. 6, 226ra32.